Nuclear Materials and Energy 37 (2023) 101548

Contents lists available at ScienceDirect

Nuclear Materials and Energy

journal homepage: www.elsevier.com/locate/nme

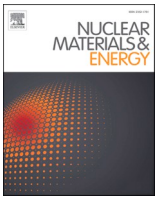

Impact of ion irradiation and film deposition on optical and fuel retention properties of Mo polycrystalline and single crystal mirrors

L. Dittrich [a,*], P. Petersson [a], H. Laabadi [a], E. Pitthan [b], M. Rubel [a,b], A. Widdowson [c], A. Krawczyńska [d], K. Szlązak [d], Ł. Ciupiński [d]

[a] KTH Royal Institute of Technology, SE-100 44 Stockholm, Sweden
[b] Uppsala University, SE-751 20 Uppsala, Sweden
[c] Culham Centre for Fusion Energy, Abingdon, OX14 3DB, United Kingdom
[d] Warsaw University of Technology, 02-507 Warsaw, Poland

ARTICLE INFO

Keywords:
Diagnostic mirrors
Ion-induced damage
Molybdenum
Helium
Boron
Reflectivity

ABSTRACT

Polycrystalline (PC) and single crystal (SC) molybdenum mirrors were irradiated with $^{98}Mo^{+}$, $^{1}H^{+}$, $^{4}He^{+}$, $^{11}B^{+}$ and $^{184}W^{+}$. Energies were chosen to impact the optically active region (up to 30 nm deep) of Mo mirrors. Some surfaces were coated by magnetron sputtering either with B or W films 4–65 nm thick. The overall objective was to simulate the neutron-induced damage and transmutation (H, He), and the impact of H, He, B, W on the optical performance of test mirrors, and on fuel retention. In parallel, a set of PC Mo mirrors irradiated with 1.6 MeV $^{98}Mo^{3+}$ to a damage of 2 dpa and 20 dpa was installed in the JET tokamak for exposure during deuterium-tritium campaigns. Data from spectrophotometric, ion beam and microscopy techniques reveal: (i) the irradiation decreased specular reflectivity, whereby the differences between PC and SC in reflectivity are very small, (ii) He is retained in bubbles within 25–30 nm of the subsurface layer in all irradiated materials, (iii) W, either deposited or implanted, decreases reflectivity, but the strongest reflectivity degradation is caused by B deposition. Laboratory studies show the correlation of damage and H retention. Several cycles of W deposition and its removal from SC-Mo mirrors by plasma-assisted methods were also performed.

Introduction

Metallic mirrors facing the plasma in diagnostic and heating systems are so-called first mirrors. At least three categories of systems will rely on them in reactor-class controlled fusion devices (CFD) to facilitate wave transmission from or to the vacuum chamber: (i) optical plasma diagnostics and imaging in the range from ultraviolet (UV) to infrared (IR) [1–5]; (ii) laser signal guiding for plasma diagnostics [6,7]; (iii) microwave injection for electron cyclotron resonance heating (ECRH) [8]. Different mirror materials will be used dependent on the purpose, but in either instance the performance will be decided by the state of reflecting surfaces. The most demanding requirements are for the diagnostic mirrors because their reliability is decisive for the safe reactor operation (machine protection), control of operation scenarios, and for advanced plasma research.

Potential threats to mirror performance have been considered for long [1,2], but the experimental program on mirror testing in tokamaks has been carried out since 2003 in carbon wall machines [4,5,9–11], and then in the metal surrounding [12–14] at JET with the ITER-like wall (JET-ILW) [15]. In parallel laboratory studies were performed [5]. The most comprehensive tests in CFD with up to 23 h of plasma operation have been carried out in JET with samples made of various materials located for exposure in different positions in the divertor, and in the main chamber using holders of diverse design [4,14]. Post-exposure studies conducted with spectrophotometry (reflectivity) and several surface analysis techniques for polycrystalline molybdenum mirrors (PC-Mo) have consistently given two sets of results. The performance of all divertor mirrors was completely lost by co-deposition (300 – 800 nm thick layers) of mainly beryllium (Be), oxygen (O) and carbon (C) with nitrogen (N), nickel (Ni) and tungsten (W). Samples from the main chamber wall maintained total reflectivity, but their surfaces contained a modified layer (extended to approximately 20 nm) containing trace amounts of Be, O, C, Ni and W embedded in Mo. The diffuse reflectivity increased from the initial 1% to 2% thus indicating some erosion by the impacting plasma species. It can be stated that all test samples, both in the divertor and the main chamber, were modified by neutral particles because of distant locations with respect to the plasma and complex structures of mirror holders.

* Corresponding author.

https://doi.org/10.1016/j.nme.2023.101548
Received 7 August 2023; Received in revised form 26 October 2023; Accepted 29 October 2023
Available online 31 October 2023

The impact of charge exchange neutrals (CXN), hydrogen (H) isotopes and particularly helium-4 (^{4}He), on the in-vessel plasma-facing diagnostic components in a deuterium–tritium (D-T) operated reactor will be significant. Simulations for ITER suggest integrated wall neutral fluxes of 3.8×10^{23} s^{-1} [16], corresponding to 4.8×10^{16} cm^{-2} s^{-1} taking into account ~800 m^2 of total main chamber wall area. ^{4}He implantation and neutron-induced effects such as damage and transmutation are to be considered in the D-T environment. Additional risks will be associated with the deposition of eroded W and, also boron (B), if boronizations are done for wall conditioning [17–19].

All above mentioned processes, including possible synergistic effects, cannot be studied in nowadays fusion machines. This motivates a test program complemented by laboratory works with ion-based simulation of neutron-induced effects such as material damage and transmutation associated with gas bubbles formation [20]. The authors are perfectly aware that the accelerator-based tests cannot fully reproduce reactor situation and deliver final answers, but they might help the assessment of potential problems and risks. Earlier works in that direction showed fairly modest impact of neutron-damage simulations by heavy ions (^{98}Mo$^+$, Zr$^+$, Nb$^+$ up to 8 dpa) on the reflectivity of PC-Mo. However, even small doses (10^{16} cm^{-2}) of H$^+$ and especially ^{4}He$^+$ decrease specular reflectivity by gas bubble accumulation thus damaging the optically active layer (OAL) [20], i.e. 20–30 nm thick outermost region. It indicates that the CXN fluxes might deposit more gaseous species than the amount generated by transmutation.

There is no decision on mirror material(s) for diagnostic systems in DEMO, however, the choice of metallic candidates is rather limited. Secondly, the effects induced by the D-T plasma species will be similar in either case. The overall objective of this work is to identify decisive factors and their possible impact on the OAL and, in consequence, on reflectivity. The specific goals are: (i) to evaluate reflectivity changes and surface/subsurface structure of PC-Mo and single crystal (SC-Mo) mirrors irradiated under same conditions; (ii) to determine the impact of W and B presence in the surface layer on the reflectivity; (iii) to assess the impact of the ion-induced damage on the retention of He and H in the mirror material. For the first time in mirror studies an experiment combining laboratory and tokamak experience with ion pre-damaged mirrors has been carried out in JET and it is introduced in the paper.

Experimental

Mirror production and reflectivity control

The study was performed with PC-Mo and SC-Mo of different crystal orientations: Mo(1 0 0), Mo(1 1 0) and Mo(1 1 1). Two types of PC-Mo mirrors were used. For laboratory studies these were 3 mm thick disks cut from a rod of 10 mm in diameter, while those for the exposure in JET-ILW were $1 \times 1 \times 1$ cm cubes with a leg for fixing in a holder; details can be found in [4]. They were ground to obtain an even surface and then polished in multiple steps to mirror finish with diamond paper, diamond paste and aluminum oxide paste with grain sizes down to 0.05 μm.

SC-Mo mirrors were cut with electro-discharge machining (EDM) from grown pieces of Mo(1 1 0) and Mo(1 1 1), the diameter was 10 mm. The Mo(1 0 0) mirror was received in disks of a diameter of roughly 12 mm. The SC-Mo mirrors were polished both mechanically and electrochemically, according to the procedure presented in [21]. The products were verified by Ion Channeling (IC) [22,23] to ensure that the SC-Mo kept their single crystalline structure on the surface.

Optical performance was determined in the wavelength range from 300 nm to 2300 nm using the dual-beam spectrophotometer Lambda 950 by Perkin Elmer, located at Uppsala University. Measurements were performed before and after ion irradiations, deposition of B and W films and an exercise of W removal. The total (R_t) and diffuse (R_d) reflectivity was recorded by placing the sample onto the opening at the integrating sphere, which is characterized by a highly reflective and diffusive white coating. The small size of the mirrors required masks with apertures of either 7 mm^2 or 16 mm^2 to mount the mirrors. Before measurements, the spectrophotometer is self-calibrated. For the measurement of R_d, the specular component exits the system by an opening in the integrating sphere. For calibrating diffuse reflectivity measurements, a dark cone acting as a perfect absorber, and a perfectly diffuse-reflective white surface were used. To measure R_t the opening remains closed, thus the specular component is included in the measurement. The calibration measurements of the perfect absorber and an aluminum mirror of known reflectivity are employed. The difference of R_t and R_d gives the specular reflectivity (R_s). It is a crucial component for mirror performance associated with the light reflected at the same angle from the mirror normal as the incident light. R_d denotes light reflected at other angles and it increases with surface roughness.

Surface modifications: Ion irradiations and film deposition

Damage by neutrons in surface/subsurface region can be simulated by the irradiation with parent ions, i.e. Mo target irradiated with Mo^{n+}. The modifications induced by such “self-irradiation” have been reported on many occasions in simulation of effects in fusion reactor materials [20]. The generation of transmutation products should be also taken into account. According to [24], the main transmutation products in Mo are Technetium (Tc, radioactive isotopes), H, Niobium (Nb), Ruthenium (Ru), Zirconium (Zr) and He. If 6.2 dpa/year are assumed for a D-T-reactor, after one year, the transmutation products roughly amount up to 40 appm He and 55 appm H [24]. Assuming a uniform distribution, in the first 20 nm of the mirror surface this would correspond to 5×10^{12} to He cm^{-2} and 7×10^{12} H cm^{-2} at the Mo density of 10.21 g/cm^3. Additionally, He from D-T reactions and hydrogen isotopes from fuel are expected to reach the mirrors, most likely as energetic CXN. This motivates shallow irradiation of Mo with H and He, and – in parallel – the introduction of B and W (by either implantation or deposition) to examine the impact of boronization and transport of W to the mirrors.

The energy of the implanted ions was chosen according to SRIM simulation [25] to generate the damage mainly in the first 20–30 nm, i.e. in the OAL, as described in [20]. The ion ranges resulting of the SRIM simulations are shown in Fig. 1. The irradiations were performed using

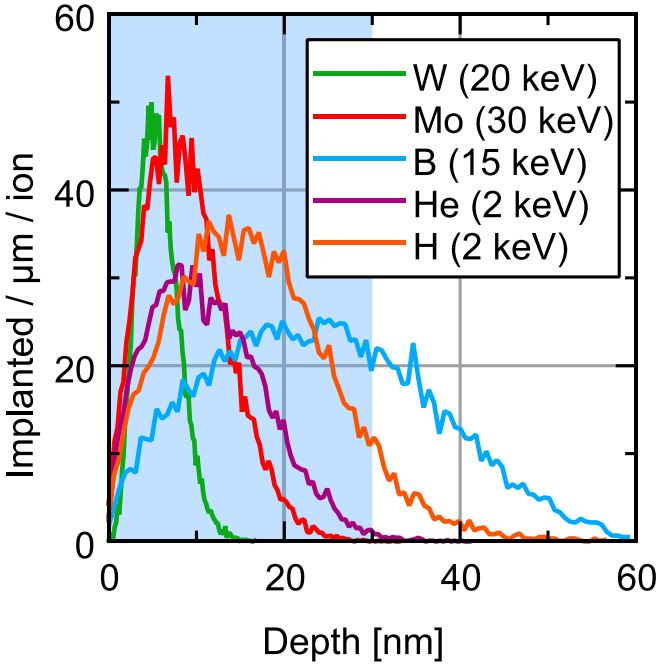

Fig. 1. Ion ranges in Mo of ^{184}W$^+$ at 20 keV, ^{98}Mo$^+$ at 30 keV, ^{11}B$^+$ at 15 keV, ^{4}He$^+$ at 2 keV and ^{1}H$^+$ at 2 keV simulated with SRIM [25].

the 350 kV Danfysik implanter, a setup is described in [26], located at the Tandem Laboratory at Uppsala University (TL-UU). The implanter operates at a standard extraction voltage of 20 kV. To achieve ion beams of lower energies, a deceleration voltage of up to 20 kV can be applied and the standard extraction potential can be changed. The 2 keV He^+ or H^+ beam is achieved by an extraction voltage of 20 kV and a deceleration voltage of 18 kV. For higher energy ion beams a maximum of 310 kV post-acceleration potential can be applied by a Cockroft-Walton multiplier [26]. The irradiated samples are oriented perpendicularly towards the incoming beam. For irradiations including SC-Mo, the samples were tilted by 7° with regard to the standard position to avoid channeling effects along crystal axes.

According to the SRIM simulations and technical capabilities of the implanter, the chosen energies of Mo^+, W^+ and B^+ were 30 keV, 20 keV and 15 keV, respectively. Plots in Fig. 1 show the ranges of the ions in Mo. Data in Table 1 provide details on the sample treatment: targets, deposited films, ions, energies, doses and the sequence of steps if irradiation was with several ions. W and B films were measured in atoms cm^{-2} and recalculated to nm by assuming the respective densities 19.29 g/cm^3 and 2.35 g/cm^3.

For magnetron-assisted sputter deposition of thin W coatings a Balzers MED 010 device was used. The working gas was argon (Ar) at the operating pressure of 1 Pa. During the deposition runs lasting for 3–200 s a series of films ranging in thickness from 4 nm to 65 nm was produced on the not irradiated PC-Mo and SC-Mo mirrors. The corresponding growth rate was around 0.3 nm/s.

The B film was prepared by radio frequency (RF) magnetron-assisted sputter deposition system, Prevac Ltd., at 13.56 MHz with Ar as the working gas. A 17 nm layer was deposited during 45 min. The growth rate was estimated to be 0.4 nm/min. The major impurities in the deposited film were O and C, 4 atomic % and 2 at. %, respectively, as determined using ion beam techniques described in next section.

Table 1
Irradiation conditions and thin film deposits of respective samples. Columns 3–5 inform about the irradiation sequence.

Sample notation	Sample material	Mo^+ 30 keV	He^+ 2 keV	Other ions Type/ Energy/Dose
1	PC-Mo	1.5×10^{15} cm^{-2}	8×10^{16} cm^{-2}	–
2A	SC-Mo(1 1 0)	1.5×10^{15} cm^{-2}	8×10^{16} cm^{-2}	–
2B	SC-Mo(1 1 1)	1.5×10^{15} cm^{-2}	8×10^{16} cm^{-2}	–
2C	SC-Mo(1 0 0)	1.5×10^{15} cm^{-2}	8×10^{16} cm^{-2}	–
3	PC-Mo with 20 nm W	–	–	–
4	PC-Mo with 17 nm B	–	–	–
5	PC-Mo	–	–	W^+ 20 keV 6.4×10^{15} cm^{-2}
6	PC-Mo	–	–	B^+ 15 keV 1.5×10^{16} cm^{-2}
7	SC-Mo(1 1 0) with 20 nm W	–	–	–
8	SC-Mo(1 1 1) with 22 to 65 nm W	–	–	–
9A	PC-Mo	–	–	H^+ 2 keV 14×10^{16} cm^{-2}
9B	PC-Mo	–	5×10^{16} cm^{-2}	H^+ 2 keV 14×10^{16} cm^{-2}
9C	PC-Mo	–	8×10^{16} cm^{-2}	H^+ 2 keV 14×10^{16} cm^{-2}
9D	PC-Mo with 4 nm W	–	–	H^+ 2 keV 14×10^{16} cm^{-2}

Material analysis with ion beam and microscopy techniques

Mirror surfaces were analyzed systematically with several methods at different stages of the experiment. Using a 5 MV pelletron tandem accelerator model 15SDH-2 by National Electrostatic Corporation at the TL-UU [26] all ion beam analyses (IBA) were performed: IC, Rutherford Backscattering Spectrometry (RBS) and Time-of-Flight Heavy Ion Elastic Recoil Detection Analysis (ToF HIERDA). Quantitative depth profiles of the H, He, B and W implants were obtained with HIERDA using an iodine-127 ($^{127}I^{10+}$) beam at the energy of 44 MeV and a ToF tube with a gas ionization chamber as the energy detector of recoiled particles, the setup is described in [27]. The detector is located at a 45° angle with respect to the incoming beam, the sample is tilted such that the beam impinges at 67.5° from the sample normal. The setup is symmetric. The beam spot on the sample is approximately 1 × 3 mm. The error of the measurement is around 10–15% for high-Z elements, mostly due to uncertainties in the stopping powers from nuclear databases. For light elements, e.g. H and He, the error can increase to around 30% caused by additional errors, most significantly the efficiency of the time-of-flight measurement. The detection limit with ToF HIERDA is at the level of 5×10^{14} atoms cm^{-2}. For RBS Passive Implanted Planar Silicon (PIPS) detectors at 170° with respect to the incoming beam were used. The error of the method is estimated at 5%. The measurements were done with a 2 MeV $^4He^+$ beam or a 3.5 MeV $^3He^+$ beam (1 mm diameter). As already stated, the polished SC-Mo mirrors were examined with IC using a 2 MeV $^4He^+$ beam.

A number of PC and SC mirrors irradiated with Mo and He were studied at the Warsaw University of Technology with Scanning Transmission Electron Microscopy (STEM) to characterize the subsurface structure including the size distribution of He bubbles. Hitachi HD2700 apparatus operated at 200 kV in bright field and Z-contrast mode was used in studies of lamellae produced by a Focused Ion Beam (FIB), Hitachi NB5000. Details of work procedure are in [28]. For each sample, at least 450 bubbles were identified. The region of interest area was chosen manually and ranged from 12 300 nm^2 to 15 900 nm^2. The images were registered with a resolution of 0.125 nm per pixel. During the semi-automated image analyses all objects equal to or smaller than 3 pixels were excluded, hence the smallest object considered for the quantitative analysis was 0.5 nm.

Recovery of reflectivity: Removal of W deposits

To check the possibility and efficiency of W deposits removal, sputtering using either an ion gun or magnetron plasma was applied. It is stressed that the aim of the exercise was only to assess whether the deposited layer can be efficiently and uniformly removed from a small surface. With the ion gun, the targets were exposed to a focused and energy filtered beam of 3 keV Ar ions with a current under 1 μA. The base pressure at the ion gun chamber is around 4×10^{-8} Pa and the operating pressure is 1×10^{-3} Pa. A W coated SC-Mo(1 1 0) mirror with a 20 nm W film was exposed in ten cleaning cycles, in total 630 min of ion gun plasma.

For the magnetron-assisted sputter treatment of the coated SC-Mo (1 1 1) mirror the Balzers MED 010 system mentioned above was used. To clean the W deposit, the mirror was installed as the sputter target, mounted in a tungsten mask. The deposition-removal cycle was performed three times. A single magnetron run lasted either 50 or 400 s.

Mirrors for exposure in JET

JET-ILW is the only device operated nowadays with the D-T fuel [29], thus creating a unique opportunity to assess the impact of damage on the change of optical properties, and on the fuel retention. In the dedicated experiment two sets of PC-Mo mirrors are exposed on the

main chamber wall during the whole campaign: (i) pre-damaged mirrors by ion irradiation; (ii) pristine mirrors serving as reference. The irradiation was performed at the Dalton Cumbrian Facility (DCF) of the University of Manchester at a 5 MV tandem Pelletron ion accelerator [30]. A 1.6 MeV $^{98}Mo^{3+}$ ion beam was used for irradiation to produce a quasi-uniform damage up to depth of 300–400 nm, as predicted by SRIM. The damage is presented in Fig. 2(a), while in Fig. 2(b) the geometry of the irradiated surfaces is presented. The damage of 2 dpa and 20 dpa was produced, according to damage calculation methods in [31]. The entire surface was irradiated first up to 2 dpa. Afterwards, a half of

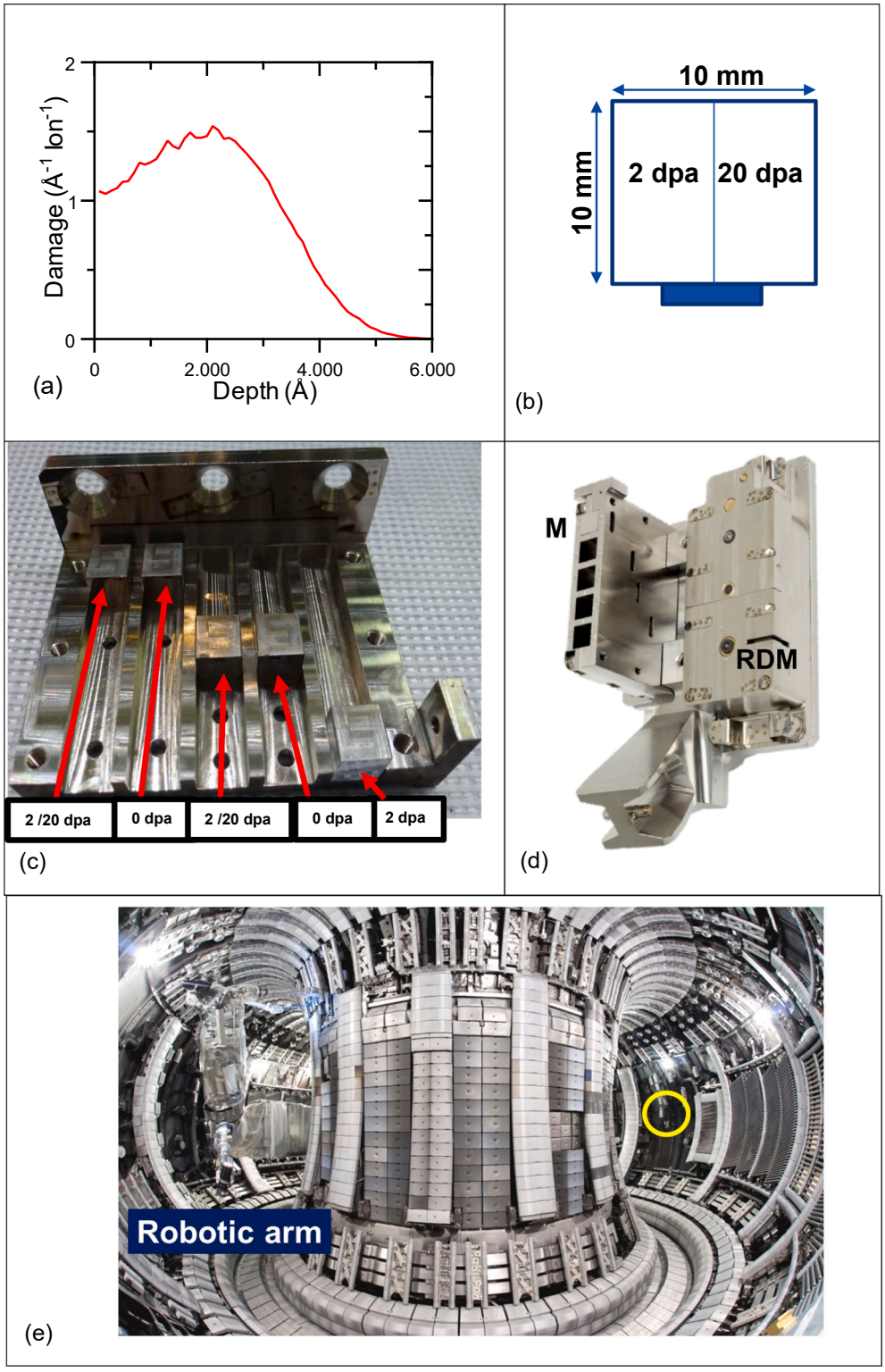

Fig. 2. (a) Damages in the self-irradiated Mo by 1.6 MeV $^{98}Mo^{3+}$ ions, as simulated by SRIM. (b) Mirror dimensions with marked surfaces irradiated to 2 and 20 dpa. (c) Five channel cassette with pre-damaged and undamaged reference Mo mirrors for exposure in JET. (d) The cassette with mirrors (M) and the rotating deposition monitor (RDM) on the wall bracket. (e) The toroidal view into JET; the yellow circle indicates the wall bracket position. (For interpretation of the references to colour in this figure legend, the reader is referred to the web version of this article.)

the area was masked and the irradiation continued up to 20 dpa. The samples were mounted in a 5-way channeled cassette, Fig. 2(c), and then placed on the wall bracket together with a rotating deposition monitor, as shown in Fig. 2(d). The whole assembly was then installed in the equatorial position of the main chamber wall; the location is marked with a circle in Fig. 2(e). Such arrangement will facilitate comparisons of morphology: (i) between the reference and irradiated test mirrors; (ii) between the exposures during the campaigns with D_2 [12,13] and the D-T campaign.

Results and Discussion

Impact of irradiation with Mo and He on PC and SC-Mo mirrors

Plots in Fig. 3 show specular reflectivity of the PC-Mo and SC-Mo (1 1 0), (1 1 1) mirrors, Samples 1, 2A and 2B, in the initial (as produced) state and after the irradiation with Mo^+ and He^+. All samples were irradiated simultaneously to ensure same conditions: 1.5×10^{15} cm^{-2} and 8×10^{16} cm^{-2} of 30 keV Mo^+ and 2 keV He^+, as detailed in Table 1.

The unirradiated SC-Mo(1 1 0) and (1 1 1) samples have very similar (nearly identical) reflectivity over the entire spectral range. The initial PC-Mo mirror performs slightly better than SC at the shorter wavelengths, 500 to 900 nm, but at the longer wavelength range its reflectivity drops by a few percent points in comparison the SC samples. The diffuse reflectivity of SC-Mo(1 1 0) and (1 1 1) is below 3% over the whole range. The diffuse reflectivity of the PC-Mo mirrors is below 3% except for the 300–430 nm range, where R_d slightly exceeds 3%.

The reflectivity of the irradiated PC and SC-Mo(1 1 0), (1 1 1) mirrors is very similar. It is also noticed that in the short wavelength range (300–800 nm) the difference between the initial and implanted samples is not significant. Around 820–1000 nm the R_s values of irradiated mirrors exceed those of the initial samples, but a strong negative impact is observed above 1000 nm, where the R_s drops by up to 12 percent points with respect to the initial level. The diffuse reflectivity does not show a tendency to increase; for the PC-Mo it even decreases below 3% in the 300 to 430 nm range.

Mirror cross-sections were subsequently analyzed with STEM; results are shown in Fig. 4. In all samples the formation of He bubbles has occurred. In the PC-Mo and SC-Mo(1 1 0) samples the bubbles reach roughly to 25 nm depth, while in SC-Mo(1 0 0), sample 2C, and SC-Mo (1 1 1) they are located in the region of up to 30 nm depth. The observed depths correspond to the SRIM simulation presented in Fig. 1. In general, the differences between respective samples are small, i.e. no clear effect of material structure (PC or SC) on the depth of the affected region can be concluded.

An observable difference is in the size distribution of the measured bubbles. In the SC-Mo(1 0 0) mirror they are of up to 2 nm diameter where more than 85% of the population is in the 0.5–1.5 nm range with the average diameter 0.8 ± 0.3 nm, as shown in Fig. 4. The bubbles in the SC-Mo(1 1 0) mirror are of up to 3 nm with a wider size distribution and an average diameter of 1.3 ± 0.5 nm. Most of the measured bubbles (68.5%) are 1.0–2.0 nm in diameter. The bubbles in the SC-Mo(1 1 1) mirror are of up to 3 nm diameter, however 2.5–3.0 nm bubbles are very rare. Close to 88% of the measured bubbles are 0.5–2.0 nm with the average diameter 0.9 ± 0.4 nm. In the PC-Mo surface the average bubble diameter is 1.4 ± 0.6 nm, which is not significantly different from the

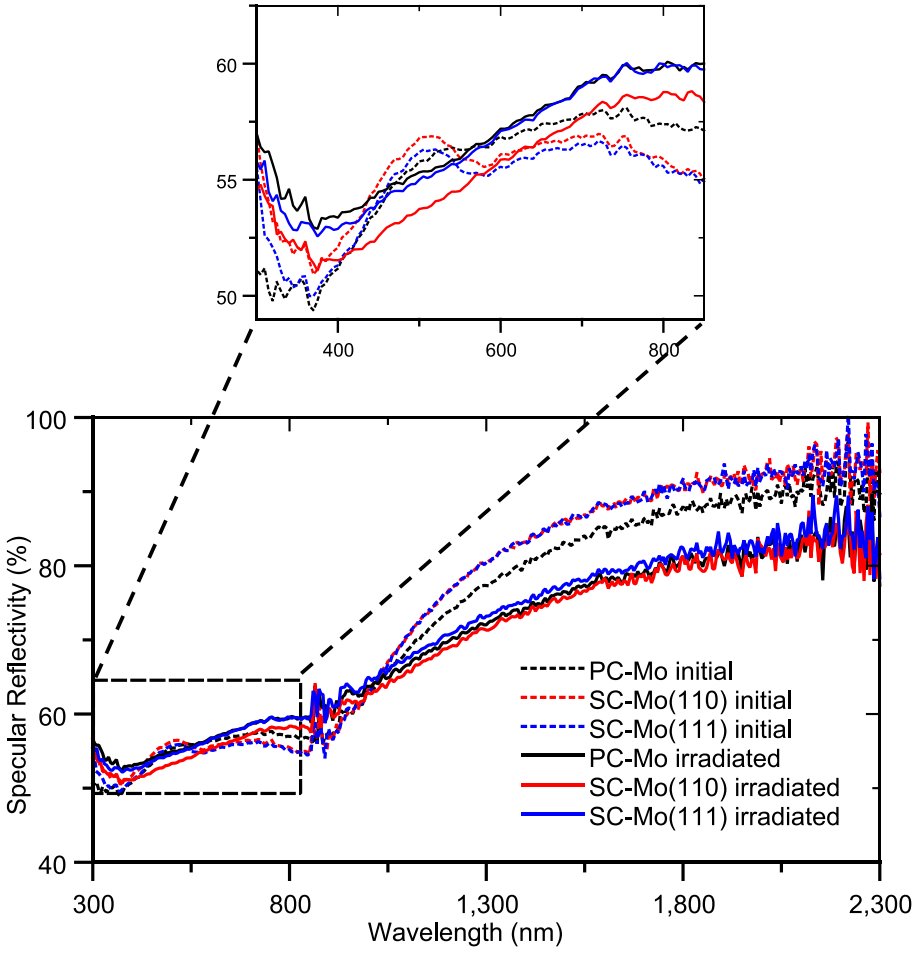

Fig. 3. Comparison of the specular reflectivity of SC-Mo and PC-Mo mirrors in the initial state and after irradiation with 1.5×10^{15} cm^{-2} and 8×10^{16} cm^{-2} of 30 keV Mo^+ and 2 keV He^+. Dotted lines represent the reflectivity of the initial mirrors and full lines those irradiated.

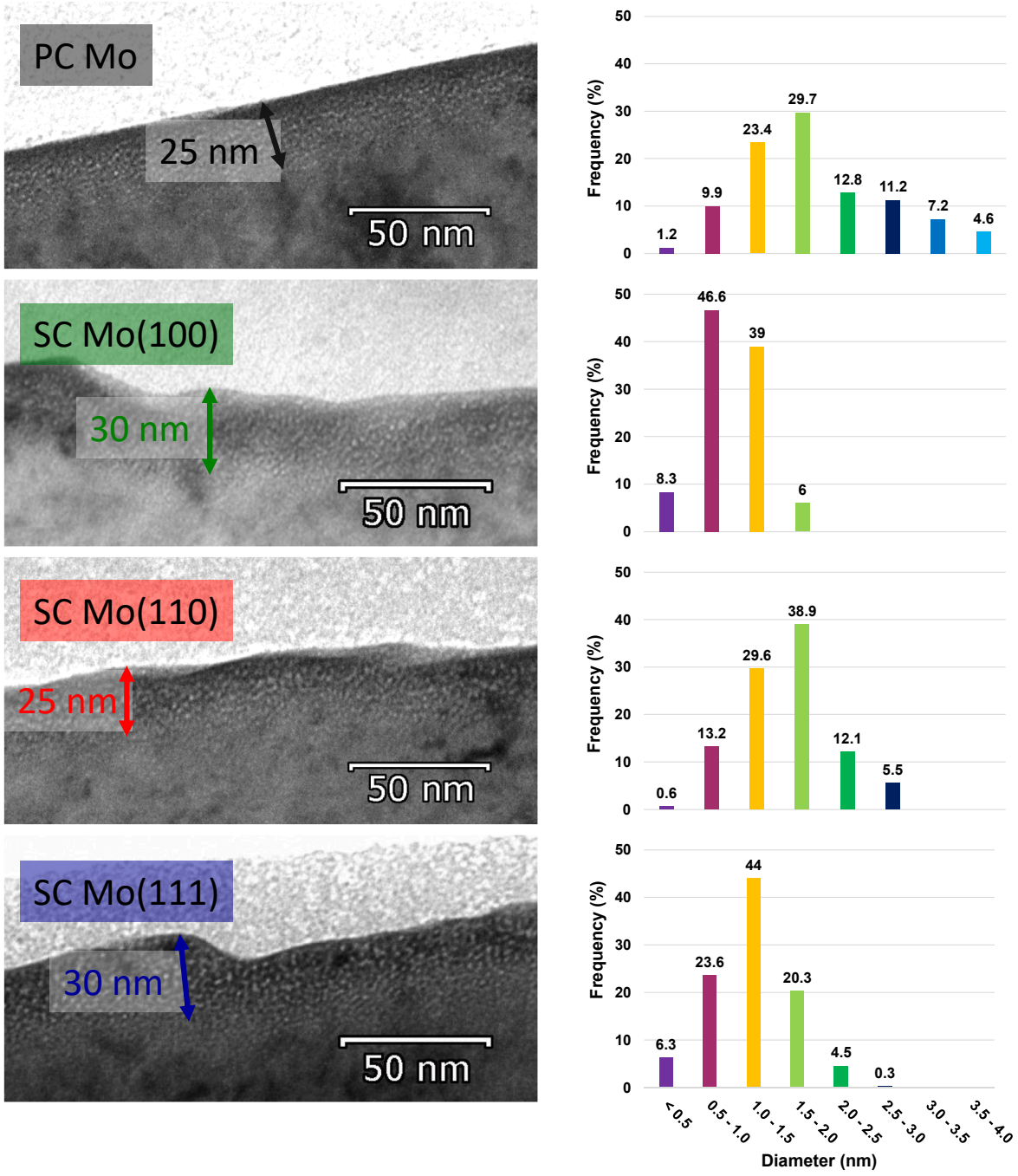

Fig. 4. Left column: STEM images of FIB-produced cross-sections of SC and PC-Mo mirrors irradiated with 1.5×10^{15} $^{98}Mo^{+}$ cm^{-2} and 8×10^{16} $^{4}He^{+}$ cm^{-2}. Right column: Corresponding size distribution of He bubbles in the mirrors.

SC-Mo mirrors. The only difference is the occurrence of 3.0–4.0 nm bubbles (12% of the population), which have not been found on any of the SC mirrors. However, once again the difference between the PC and SC is small, and it is too risky to discuss, whether this would have a significant impact on material properties including the optical performance.

Tungsten and boron impact on reflectivity of Mo mirrors

In a boronized full tungsten surrounding, B and W species eroded from the wall may reach mirrors in some locations, especially in the divertor. This would lead to the formation of B- and W-containing co-deposited and/or co-implanted layers. Both cases have been simulated under laboratory conditions. W films of different thicknesses and a B film were deposited by a magnetron plasma on several poly- and single crystal mirrors. Reflectivity plots in Fig. 5 have been obtained for the pristine PC-Mo mirrors in the initial state and after the magnetron-assisted deposition of the 20 nm W film, Sample 3, and the deposition of the 17 nm B film on a separate mirror, Sample 4. For the W film, reflectivity has decreased over the entire range by 5 to 30 percent points. Even a 3.5 nm thick W layer deposited on the surface starts having an impact on optical performance, as it was presented in [28]. The B layer has in the optical range 300–1050 nm an even stronger impact on R_S than the W layer. At the wavelength of 460 nm the reflectivity decreased to 10%. However, in the 1800–2300 nm range, the reflectivity decreases only by a few percent points. To our knowledge, these are the first

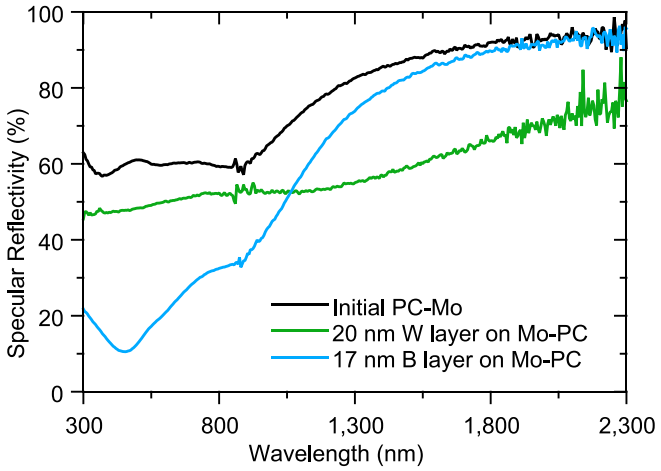

Fig. 5. Specular reflectivity of the initial PC-Mo mirror, mirror 3 with 20 nm W coating, and mirror 4 with a 17 nm B coating, both deposited by magnetron sputtering.

reflectivity measurements of boron coatings.

In the erosion-dominated case, a shallow co-implantation of various species (including W) may occur, as noticed earlier in the First Mirror Test in JET-ILW [12]. To verify the influence of tungsten and boron (in the case of a boronized machine) on the OAL two PC-Mo mirrors, Samples 5 and 6, were implanted in separate runs with those ions. The results in Fig. 6 indicate fairly small impact in the wavelength range up to 1100 nm; there are only some reflectivity variations within approximately 3 percent points. Degradation of the optical performance is evident in the range above 1100 nm and it is on the same level for both species. It should be stressed that such effects are triggered already with very small doses: 1.5×10^{16} B cm^{-2} and 6.4×10^{15} W cm^{-2}. Both numbers would correspond to 1.2 nm and 1.0 nm thick layers, respectively, if the elements were deposited on surfaces.

The implanted mirrors were examined with HIERDA to quantify W and B, and to detect the presence of other species, especially low-Z impurities always occurring in laboratory systems. Depth profiles are shown in Fig. 7. The distribution of W is narrow and peaked with a maximum at 5–15 nm thus being in good agreement with the SRIM-based predictions from Fig. 1. A perfect match cannot be expected because predictions are for an ideal target structure, while experiments are done on real materials with some imperfections. The total W content measured with HIERDA amounts to 7.1×10^{15} W cm^{-2}. This slightly

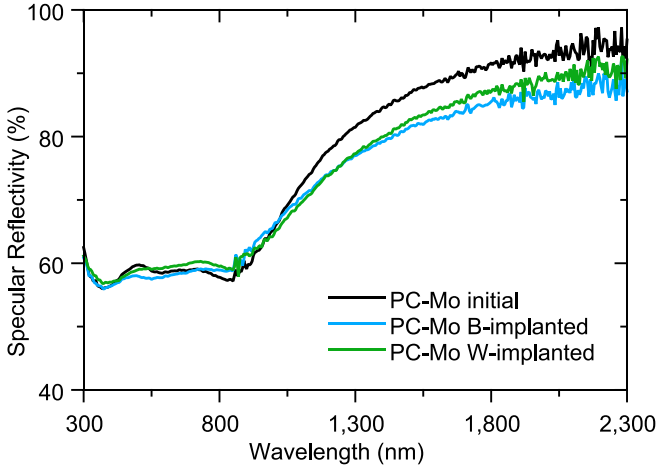

Fig. 6. Specular reflectivity of the initial PC-Mo mirror and mirrors irradiated either with 6.4×10^{15} W$^+$ at 20 keV, mirror 5, or 1.5×10^{16} B$^+$ at 15 keV, mirror 6.

overestimated result is in line with the expected complete retention of the implanted W, combined with dual scattering effects in the sample, which are common for heavy species and increase the likelihood of detection. The boron distribution is broad and fairly uniform. With some fluctuations it reaches the depth of 100 nm, i.e. it is greater than the 60 nm predicted by SRIM. It may be very tentatively suggested that such profile broadening is related to the formation of molybdenum boride (MoB, Mo_2B, Mo_2B_5), but any further speculations must be avoided, because some processes like diffusion under irradiation cannot be fully excluded. The total content of B retained in the mirror is 1.1×10^{16} cm^{-2}, being equal to 73% of the implanted amount. As expected, the main surface impurities are carbon and oxygen, in total below 7×10^{15} cm^{-2}.

The two experimental approaches do not and cannot fully simulate the situation in a tokamak. However, they clearly indicate that: (i) a shallow implantation of B and/or W into a surface under erosion conditions will have a minor impact on optical properties; (ii) the formation of a deposited/co-deposited layers (especially B-rich) will lead to a major degradation of mirror performance.

Removal of W films: Recovery of reflectivity

The magnetron deposited W layer on the SC-Mo(1 1 0) mirror, Sample 7, was treated for 630 min with a 3 keV Ar^+ beam from the ion gun to remove a layer of 125×10^{15} atoms cm^{-2}, corresponding to 20 nm. Reflectivity measurements at two different points on the mirror provided different results: either full or partial reflectivity recovery. The original W amount of 125×10^{15} atoms cm^{-2} was reduced to 2×10^{15} atoms cm^{-2}, 34×10^{15} atoms cm^{-2}, and 64×10^{15} atoms cm^{-2} in three points examined with RBS. The measurements indicate an inhomogeneous removal of W residues even from such a small mirror surface.

Magnetron-assisted treatment to recover reflectivity of the SC-Mo (1 1 1) mirror, Sample 8, coated trice by W, is summarized in Table 2. While cycle #1 and #3 managed to recover reflectivity while leaving only small W residues (0.6×10^{15} and 1.3×10^{15} atoms cm^{-2}), which would correspond to layers of 0.1 or 0.2 nm. The short cycle #2 only partially removed W and the specular reflectivity was not recovered, see Fig. 8. Results from cycles #1 and #3 indicate fair efficiency of the method on laboratory-deposited W layers. However, that positive fact does not allow any further conclusions regarding the fate of mirrors exposed in a metal-wall tokamak, as it has been shown with radio frequency methods that reflectivity recovery of mirrors from JET-ILW is challenging [32], but a comprehensive research on mirror cleaning is in progress [33–35].

Ion damaged mirrors for JET: Optical and fuel retention studies

The PC-Mo mirrors were irradiated with 1.6 MeV $^{98}Mo^{3+}$ ions to produce damage extending up to 400 nm to enable optical and fuel retention studies after the D-T campaign. The specular reflectivity is shown in Fig. 9, where the data for the initial PC-Mo mirror are compared with those for damaged targets at 2 dpa and 20 dpa. The reflectivity decreased only slightly with 2 dpa, while the bigger damage with 20 dpa caused R_s to drop by 5 to 10 percent points; the strongest effect is in the short wavelength range. The diffuse reflectivity increased from around 0.5% to 1–2% at 20 dpa.

Post-exposure analyses of mirrors from JET-ILW may become possible a few years after termination of the D-T campaigns and machine clean-up phases to reduce the in-vessel tritium content. Therefore, in parallel to that long-term program, the impact of ion-induced damage on the retention in PC-Mo has been examined. Mirrors were irradiated with H^+, two of them pre-irradiated with different He^+ doses, details for Samples 9A – 9D are in Table 1. A series of plots in Fig. 10 show the evolution of H and He depth profiles measured with HIERDA. The profile of hydrogen implanted into a PC-Mo is peaked in the near surface region at the depth around 15 nm, as predicted by SRIM see Fig. 1. However,

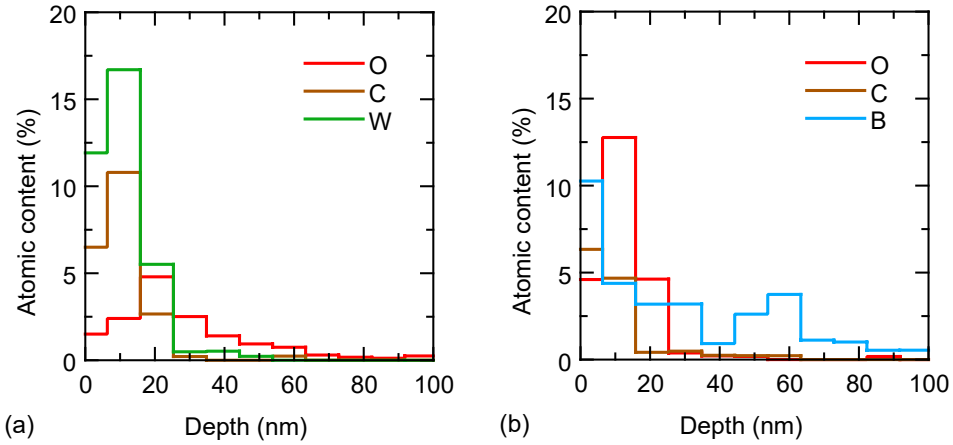

Fig. 7. Quantitative HIERDA depth profiles of elements present in the Mo mirrors implanted with: (a) tungsten, mirror 5, and (b) boron, mirror 6. The amounts are given in atomic percent.

Table 2
Magnetron-assisted sputter cleaning cycles to recover the SC-Mo(1 1 1) after W film deposits.

Cleaning cycle	Exposure time [s]	W layer before exposure [10^{15} atoms cm^{-2}]	W layer after exposure [10^{15} atoms cm^{-2}]
#1	400	140	0.6
#2	50	390	200
#3	400	410	1.3

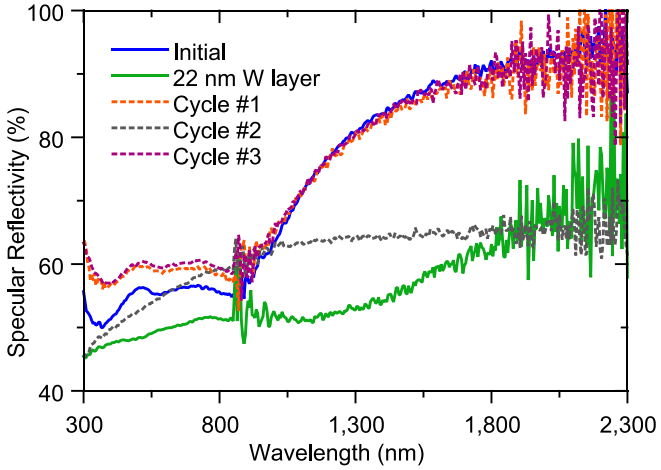

Fig. 8. Specular reflectivity of the initial polished SC-Mo(1 1 1) mirror, the mirror with the deposited W layer of 140 × 10^{15} atoms cm^{-2}, corresponding to 22 nm, and the recovered mirror after the cleaning cycles #1, #2 and #3 in dotted lines.

when the implantation of the same H dose (14 × 10^{16} cm^{-2}) is done into the target pre-damaged also with 5 × 10^{16} cm^{-2} of He, the profile flattens near the surface and broadens into the bulk, see Fig. 10(a). In addition, the amount of H retained after the implantation increases by a factor of 2 from 2 at.% to 4 at.%. The flattening and broadening of the H profile continues with the He dose increase to 8 × 10^{16} cm^{-2}, and the H retention still increases to 5 at.%, as is shown in Fig. 10(b). The deposition of 25 × 10^{15} W cm^{-2}, corresponding to a 4 nm thick W layer, on the PC-Mo mirror reduces the fraction of the retained H in comparison to the not coated surface: 1 at.% in sample 9D versus 2 at.% in 9A, see Fig. 10(c).

The data obtained indicate the direction of changes even under small doses. In addition to the serious influence of He irradiation on the optical

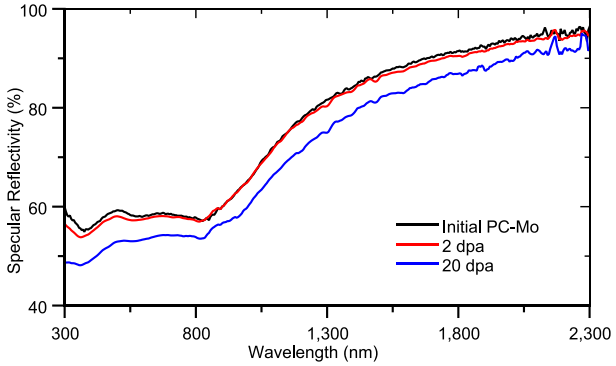

Fig. 9. Specular reflectivity measured on the undamaged and pre-damaged PC-Mo mirrors with 2 dpa and 20 dpa.

performance, the data show an impact on fuel retention properties of the exposed components.

Concluding remarks

Reliable performance of first mirrors will be crucial in reactor safety and plasma research as long as the use of such optical components is planned in the next-step devices, both ITER and various DEMO concepts. All data obtained until now in current machines show that CXN and wall composition are decisive for the state of first mirrors. Supporting laboratory-based research [5,20] and modelling of CXN fluxes [16] help identification of issues and topics for further research. They may also indicate ways towards solutions.

This work has provided two major contributions to the field: (i) behavior of PC versus SC under ion irradiation; (ii) impact of B (first-ever studies) and W on reflectivity. Comparative studies of poly-crystalline and single crystal Mo mirrors damaged by self-irradiation with Mo^+ and He^+ have identified only small differences in the optical performance and surface state of respective test samples. One may expect similar behavior of both types of Mo materials under reactor conditions.

Co-deposition and co-implantation of tungsten will occur in a long-pulse or a steady-state reactor. The data from deposition and implantation experiments indicate that such W deposition is a significant threat for optical properties. Decisively more serious effects are associated with the B deposition degrading optical properties, while fairly significant boron fluxes will occur in a boronized full W surrounding. It is stressed that these are early data on the boron impact on mirrors, while

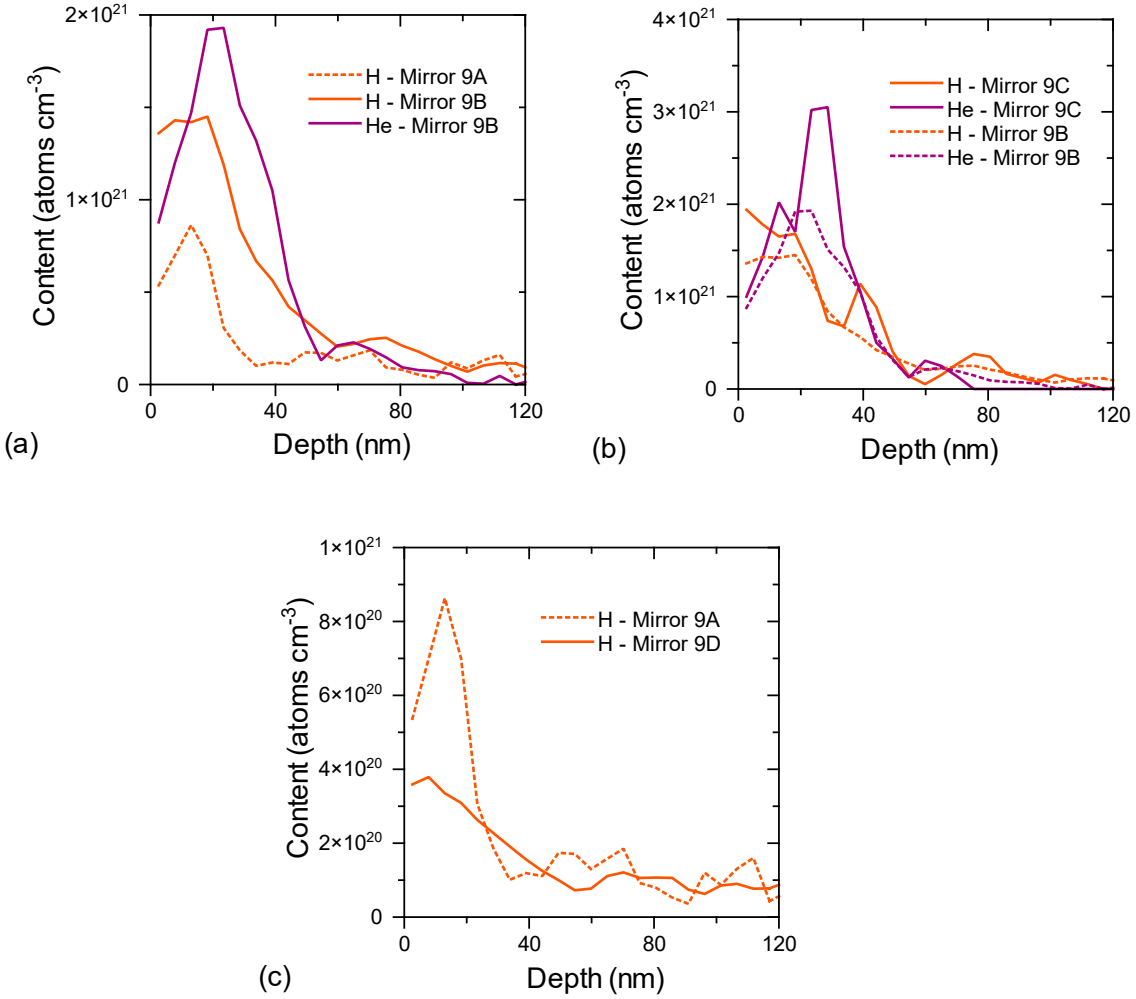

Fig. 10. He and H depth profiles after irradiation measured with HIERDA. (a) Mirror 9A irradiated with 14×10^{16} H cm^{-2} and mirror 9B irradiated with 5×10^{16} He cm^{-2} and subsequently with 14×10^{16} H cm^{-2}. (b) Mirror 9B for comparison and mirror 9C irradiated with 8×10^{16} He cm^{-2} and subsequently with 14×10^{16} H cm^{-2}. (c) Mirror 9A for comparison and mirror 9D coated with 25×10^{15} W cm^{-2} and irradiated with 14×10^{16} H cm^{-2}.

synergistic effects of W and B cannot be excluded. It may be deemed, however, that the low-Z species (H isotopes, He and B) will become decisive species for compositional changes in the surface region, i.e. OAL.

The experience gained for tokamak activities and laboratory systems is merged in the unique experiment carried out in JET-ILW. The currently installed mirrors serve both for optical tests and, as deposition monitors in fuel retention studies. The laboratory data in Section 3.4 show the correlation of damage and retention. One understands that laboratory experiments may not quantitatively reflect the reactor scenario, but the tendency of property changes in damaged and He irradiated materials is clearly indicated.

CRediT authorship contribution statement

L. Dittrich: Methodology, Validation, Formal analysis, Investigation, Writing – original draft, Writing – review & editing, Visualization. **P. Petersson:** Conceptualization, Methodology, Validation, Formal analysis, Investigation, Writing – review & editing, Supervision, Funding acquisition, Project administration. **H. Laabadi:** Methodology, Validation, Formal analysis, Investigation. **E. Pitthan:** Methodology, Investigation, Resources. **M. Rubel:** Conceptualization, Writing – original draft, Writing – review & editing, Supervision, Funding acquisition, Project administration. **A. Widdowson:** Conceptualization, Funding acquisition, Project administration. **A. Krawczyńska:** Methodology, Investigation. **K. Szlązak:** Methodology, Formal analysis, Investigation. **Ł. Ciupiński:** Methodology, Investigation.

Declaration of Competing Interest

The authors declare that they have no known competing financial interests or personal relationships that could have appeared to influence the work reported in this paper.

Data availability

Data will be made available on request.

Acknowledgements:

This work has been carried out within the framework of the EUROfusion Consortium, funded by the European Union via the Euratom Research and Training Programme (Grant Agreement No 101052200 — EUROfusion). Views and opinions expressed are however those of the author(s) only and do not necessarily reflect those of the European Union or the European Commission. Neither the European Union nor the European Commission can be held responsible for them. The work has been supported by the Swedish Research Council (VR) [Grant 2015–04844 and 2016-05380]. Financial support of the Tandem Accelerator Infrastructure by VR-RFI [Grant 2017–00646_9,

2019_00191] as well as the Swedish Foundation for Strategic Research (SSF) under contract RIF14–0053 is gratefully acknowledged. The authors of Warsaw University of Technology acknowledge financial contribution of the Ministry of Education and Science through the PMW program in 2022, agreement No. 5257/HEU-EURATOM/2022/2.

References

[1] A.E. Costley, D.J. Campbell, S. Kasai, K.E. Young, V. Zaveriaev, ITER R&D: Auxiliary Systems: Plasma Diagnostics, Fusion Eng. Des. 55 (2001) 331–346, https://doi.org/10.1016/S0920-3796(01)00200-9.

[2] V.S. Voitsenya, A.F. Bardamid, V.N. Bondarenko, W. Jacob, V.G. Konovalov, S. Masuzaki, O. Motojima, D.V. Orlinskij, V.L. Poperenko, I.V. Ryzhkov, A. Sagara, A.F. Shtan, S.I. Solodovchenko, M.V. Vinnichenko, Some problems arising due to plasma–surface interaction for operation of the in-vessel mirrors in a fusion reactor, J. Nucl. Mater. 290–293 (2001) 336–340, https://doi.org/10.1016/S0022-3115(00)00634-6.

[3] A.E. Costley, T. Sugie, G. Vayakis, C.I. Walker, Technological challenges of ITER diagnostics, Fusion Eng. Des. 74 (2005) 109–119, https://doi.org/10.1016/j.fusengdes.2005.08.026.

[4] M.J. Rubel, G. De Temmerman, J.P. Coad, J. Vince, J.R. Drake, F. Le Guern, A. Murari, R.A. Pitts, C. Walker, Jet-Efda Contributors, Mirror test for International Thermonuclear Experimental Reactor at the JET tokamak: An overview of the program, Rev. Sci. Instrum. 77 (2006), 063501, https://doi.org/10.1063/1.2202915.

[5] A. Litnovsky, V.S. Voitsenya, R. Reichle, M. Walsh, A. Razdobarin, A. Dmitriev, N. Babinov, L. Marot, L. Moser, R. Yan, M. Rubel, A. Widdowson, S. Moon, S.G. Oh, Y. An, P. Shigin, I. Orlovskiy, K.Y. Vukolov, E. Andreenko, A. Krimmer, V. Kotov, P. h. Mertens, Specialists Working Group on First Mirrors of the ITPA Topical Group on Diagnostics, Diagnostic mirrors for ITER: research in the frame of International Tokamak Physics Activity, Nucl. Fusion 59 (2019), 066029, https://doi.org/10.1088/1741-4326/ab1446.

[6] A. Huber, B. Schweer, V. Philipps, N. Gierse, M. Zlobinski, S. Brezinsek, W. Biel, V. Kotov, R. Leyte-Gonzales, P.h. Mertens, U. Samm, Development of laser-based diagnostics for surface characterisation of wall components in fusion devices, Fusion Eng. Des. 86 (2011) 1336–1340, https://doi.org/10.1016/j.fusengdes.2011.01.090.

[7] M. Bassan, P. Andrew, G. Kurskiev, E. Mukhin, T. Hatae, G. Vayakis, E. Yatsuka, M. Walsh, Thomson scattering diagnostic systems in ITER, J. Inst. 11 (2016) C01052–C, https://doi.org/10.1088/1748-0221/11/01/C01052.

[8] M.F. Graswinckel, W.A. Bongers, M.R. De Baar, M.A. Van Den Berg, G. Denisov, A. J.H. Donné, B.S.Q. Elzendoorn, A.P.H. Goede, R. Heidinger, S. Kuzikov, O.G. Kruijt, B. Kruizinga, A. Moro, E. Poli, D.M.S. Ronden, G. Saibene, D.J. Thoen, A.G. A. Verhoeven, Advanced launcher design options for electron cyclotron current drive on ITER based on remote steering, Nucl. Fusion. 48 (2008), 054015, https://doi.org/10.1088/0029-5515/48/5/054015.

[9] P. Wienhold, A. Litnovsky, V. Philipps, B. Schweer, G. Sergienko, P. Oelhafen, M. Ley, G. De Temmerman, W. Schneider, D. Hildebrandt, M. Laux, M. Rubel, B. Emmoth, Exposure of metal mirrors in the scrape-off layer of TEXTOR, J. Nucl. Mater. 337–339 (2005) 1116–1120, https://doi.org/10.1016/j.jnucmat.2004.09.047.

[10] M. Lipa, B. Schunke, C.h. Gil, J. Bucalossi, V.S. Voitsenya, V. Konovalov, K. Vukolov, M. Balden, G. De Temmerman, P. Oelhafen, A. Litnovsky, P. Wienhold, Analyses of metallic first mirror samples after long term plasma exposure in Tore Supra, Fusion Eng. Des. 81 (2006) 221–225, https://doi.org/10.1016/j.fusengdes.2005.07.017.

[11] M. Rubel, G.D. Temmerman, P. Sundelin, J.P. Coad, A. Widdowson, D. Hole, F. L. Guern, M. Stamp, J. Vince, An overview of a comprehensive First Mirror Test for ITER at JET, J. Nucl. Mater. 390–391 (2009) 1066–1069, https://doi.org/10.1016/j.jnucmat.2009.01.257.

[12] D. Ivanova, M. Rubel, A. Widdowson, P. Petersson, J. Likonen, L. Marot, E. Alves, A. Garcia-Carrasco, G. Pintsuk, J.P. Coad, An overview of the comprehensive First Mirror Test in JET with ITER-like wall, Phys. Scr. T159 (2014), 014011, https://doi.org/10.1088/0031-8949/2014/T159/014011.

[13] S. Moon, P. Petersson, M. Rubel, E. Fortuna-Zalesna, A. Widdowson, S. Jachmich, A. Litnovsky, E. Alves, First mirror test in JET for ITER: Complete overview after three ILW campaigns, Nuclear Materials and Energy. 19 (2019) 59–66, https://doi.org/10.1016/j.nme.2019.02.009.

[14] M. Rubel, S. Moon, P. Petersson, A. Widdowson, R.A. Pitts, S. Aleiferis, E. Fortuna-Zaleśna, G.D. Temmerman, R. Reichle, First mirror erosion–deposition studies in JET using an ITER-like mirror test assembly, Nucl. Fusion 61 (2021), 046022, https://doi.org/10.1088/1741-4326/abdb92.

[15] G.F. Matthews, M. Beurskens, S. Brezinsek, M. Groth, E. Joffrin, A. Loving, M. Kear, M.-L. Mayoral, R. Neu, P. Prior, V. Riccardo, F. Rimini, M. Rubel, G. Sips, E. Villedieu, P. de Vries, M.L. Watkins, EFDA-JET contributors, JET ITER-like wall—overview and experimental programme, Phys. Scr. T145 (2011), 014001, https://doi.org/10.1088/0031-8949/2011/T145/014001.

[16] J. Romazanov, S. Brezinsek, A. Kirschner, D. Borodin, A. Eksaeva, R.A. Pitts, S. W. Lisgo, H. Anand, E. Veshchev, V.S. Neverov, A.B. Kukushkin, A.G. Alekseev, C. Linsmeier, First Monte-Carlo modelling of global beryllium migration in ITER using ERO2.0, Contrib. Plasma Phys. 60 (2020), e201900149, https://doi.org/10.1002/ctpp.201900149.

[17] J. Winter, H.G. Esser, L. Könen, V. Philipps, H. Reimer, J.V. Seggern, J. Schlüter, E. Vietzke, F. Waelbroeck, P. Wienhold, T. Banno, D. Ringer, S. Vepřek, Boronization in TEXTOR, J. Nucl. Mater. 162–164 (1989) 713–723, https://doi.org/10.1016/0022-3115(89)90352-8.

[18] J. Bucalossi, et al., Operating a full tungsten actively cooled tokamak: overview of WEST first phase of operation, Nucl. Fusion. 62 (2022), 042007, https://doi.org/10.1088/1741-4326/ac2525.

[19] M. Dibon, V. Rohde, F. Stelzer, K. Hegele, M. Uhlmann, New boronization system at ASDEX Upgrade, Fusion Eng. Des. 165 (2021), 112233, https://doi.org/10.1016/j.fusengdes.2021.112233.

[20] A. Garcia-Carrasco, P. Petersson, A. Hallén, J. Grzonka, M.R. Gilbert, E. Fortuna-Zalesna, M. Rubel, Impact of helium implantation and ion-induced damage on reflectivity of molybdenum mirrors, Nucl. Instrum. Methods Phys. Res., Sect. B 382 (2016) 91–95, https://doi.org/10.1016/j.nimb.2016.02.065.

[21] M. Zamin, P. Mayer, M.K. Murthy, On the Electropolishing of Molybdenum, J. Electrochem. Soc. 124 (1977) 1558, https://doi.org/10.1149/1.2133110.

[22] J.W. Mayer, E. Rimini (Eds.), Ion beam handbook for material analysis, Academic Press, New York, 1977.

[23] D.V. Morgan, Channeling: theory, observation and applications, Wiley, London, New York, 1973.

[24] M.R. Gilbert, J.-C. Sublet, Handbook of activation, transmutation, and radiation damage properties of the elements simulated using FISPACT-II & TENDL-2015; Magnetic Fusion Plants, UK Atomic Energy Authority, Culham Science Centre, Abingdon, Oxfordshire, UK, 2016. https://fispact.ukaea.uk/wp-content/uploads/2016/10/CCFE-R1636.pdf.

[25] J.F. Ziegler, M.D. Ziegler, J.P. Biersack, SRIM – The stopping and range of ions in matter (2010), Nucl. Instrum. Methods Phys. Res., Sect. B 268 (2010) 1818–1823, https://doi.org/10.1016/j.nimb.2010.02.091.

[26] P. Ström, D. Primetzhofer, Ion beam tools for nondestructive in-situ and in-operando composition analysis and modification of materials at the Tandem Laboratory in Uppsala, J. Inst. 17 (2022) P04011, https://doi.org/10.1088/1748-0221/17/04/P04011.

[27] P. Ström, P. Petersson, M. Rubel, G. Possnert, A combined segmented anode gas ionization chamber and time-of-flight detector for heavy ion elastic recoil detection analysis, Rev. Sci. Instrum. 87 (2016), 103303, https://doi.org/10.1063/1.4963709.

[28] A.T. Krawczynska, Ł. Ciupiński, P. Petersson, Impact of material migration and radiation damage on the reflectivity of molybdenum mirrors: laboratory test for DEMO, Phys. Scr. T171 (2020), 014019, https://doi.org/10.1088/1402-4896/ab3e81.

[29] J. Mailloux, et al., Overview of JET results for optimising ITER operation, Nucl. Fusion 62 (2022) 042026, https://doi.org/10.1088/1741-4326/ac47b4.

[30] P.T. Wady, A. Draude, S.M. Shubeita, A.D. Smith, N. Mason, S.M. Pimblott, E. Jimenez-Melero, Accelerated radiation damage test facility using a 5 MV tandem ion accelerator, Nucl. Instrum. Methods Phys. Res., Sect. A 806 (2016) 109–116, https://doi.org/10.1016/j.nima.2015.09.088.

[31] S. Agarwal, Y. Lin, C. Li, R.E. Stoller, S.J. Zinkle, On the use of SRIM for calculating vacancy production: Quick calculation and full-cascade options, Nucl. Instrum. Methods Phys. Res., Sect. B 503 (2021) 11–29, https://doi.org/10.1016/j.nimb.2021.06.018.

[32] L. Moser, L. Marot, R. Steiner, M. Newman, A. Widdowson, D. Ivanova, J. Likonen, P. Petersson, G. Pintsuk, M. Rubel, E. Meyer, J. Contributors, Plasma cleaning of beryllium coated mirrors, Phys. Scr. T167 (2016), 014069, https://doi.org/10.1088/0031-8949/T167/1/014069.

[33] M. Ben Yaala, L. Moser, R. Steiner, B. Butoi, P. Dinca, P. Petersson, L. Marot, E. Meyer, Deuterium as a cleaning gas for ITER first mirrors: experimental study on beryllium deposits from laboratory and JET-ILW, Nucl. Fusion. 59 (2019), 096027, https://doi.org/10.1088/1741-4326/ab2d31.

[34] K. Soni, S. Iyyakkunnel, R. Steiner, R. Antunes, L. Moser, O. Bieri, L. Marot, E. Meyer, Effect of 3 T magnetic field on RF plasma sputtering in an ITER-relevant first mirror unit, Nucl. Fusion. 62 (2022), 126009, https://doi.org/10.1088/1741-4326/ac8b20.

[35] P. Shigin, N. Babinov, G. De Temmerman, A. Danisi, A. Dmitriev, J. Larsen, R. Madsen, L. Marot, L. Moser, E. Mukhin, M. Kochergin, R. Ortiz, A. Razdobarin, R. Reichle, R. Pitts, D. Samsonov, M. Tsalas, V. Udintsev, G. Vayakis, M. Walsh, RF discharge mirror cleaning system development for ITER diagnostics, Fusion Eng. Des. 164 (2021), 112162, https://doi.org/10.1016/j.fusengdes.2020.112162.